Aging and Disease
www.aginganddisease.org
Early access date: February 20, 2026
http://dx.doi.org/10.14336/AD.2026.10202

Original Article

Danggui-Shaoyao San Promotes Microglia-Mediated Oligodendrocyte Maturation and White Matter Repair After Stroke

Fang Tong[1], Yihan Liu[1], Nan Deng[1], Yong Yang[2], Sijie Li[1], Ziping Han[1], Jingfei Shi[3], Xunming Ji[1], Changhong Ren[1*]

[1]Beijing Key Laboratory of Hypoxia Conditioning Translation Medicine, Xuanwu Hospital, Capital Medical University, Beijing, China. [2]School of Chinese Medicine, Beijing University of Chines Medicine, Beijing, China. [3]China-America Institute of Neurology, Xuanwu Hospital, Capital Medical University, Beijing, China.

[Received November 5, 2025; Revised February 16, 2026; Accepted February 17, 2026]

ABSTRACT: Ischemic stroke is a leading cause of long-term disability, yet effective therapies that promote white matter repair and remyelination during the recovery phase remain limited. Danggui-Shaoyao-San (DSS) has demonstrated neuroprotective effects, but its mechanisms during the recovery phase are unclear. Here, we tested whether delayed DSS treatment improves long-term outcomes after transient focal ischemia by reprogramming microglia to support oligodendroglial differentiation and remyelination. In a mouse model of transient middle cerebral artery occlusion, DSS starting 30 min after reperfusion and continued throughout the recovery period produced sustained improvements in neurological function. These benefits were accompanied by preserved myelin-axon coupling, improved myelin ultrastructure in peri-infarct white matter, and enhanced progression of oligodendrocyte lineage cells toward a mature myelin-forming state. DSS reduced pro-inflammatory microglial activation while increasing repair associated microglial markers across the subacute period. Mechanistically, DSS enhanced microglial estrogen receptor ERα and ERβ signaling, increased expression of the ER associated corepressor CtBP, and suppressed NF-κB activation. In BV2 microglia, DSS containing serum dampened LPS-induced inflammatory gene expression programs and promoted repair associated markers, and pharmacological ER blockade reversed DSS-driven microglial polarization. Importantly, conditioned medium from DSS-treated microglia rather than direct exposure to DSS promoted oligodendroglial differentiation and induced pro-regenerative gene expression in oligodendrocyte lineage cells, supporting a paracrine signaling mechanism from microglia to oligodendroglia. Together, our findings identify DSS as a delayed recovery phase intervention that improves long term outcomes after ischemic stroke and suggest that ER dependent microglial reprogramming is a tractable upstream target for promoting remyelination and white matter repair.

Keywords: Danggui-Shaoyao-San (DSS), ischemic stroke, microglia polarization, estrogen receptor (ER), white matter repair

INTRODUCTION

Ischemic stroke remains a leading cause of death and long-term disability worldwide. Despite major advances in acute reperfusion therapies, a large proportion of survivors experience persistent neurological deficits driven not only by neuronal loss, but also by secondary injury processes that evolve over days to weeks [1, 2]. Among these delayed processes, white matter injury, including demyelination, axonal degeneration, and impaired remyelination, has emerged as a key determinant of chronic cognitive and motor dysfunction [3]. Remyelination depends largely on oligodendrocyte lineage progression, yet the post-stroke environment often

***Correspondence should be addressed to:** Dr. Changhong Ren, Beijing Key Laboratory of Hypoxia Conditioning Translation Medicine, Xuanwu Hospital, Capital Medical University, 100053, China. Email: rench@xwhosp.org.

constrains oligodendrocyte precursor cell (OPC) maturation, limiting structural and functional recovery [4]. Thus, recovery-phase strategies that actively promote white matter restoration remain an important but still clinically underdeveloped therapeutic direction

Microglia are strategically positioned to influence this repair trajectory. Following ischemia, microglia rapidly activate and adopt heterogeneous phenotypes that span injury-amplifying programs and repair-associated programs [5]. Notably, studies have reported that enhancing the activity of tissue repair-type microglia upregulates pro-oligodendrogenic cytokine expression within microglia, thereby promoting oligodendrocyte regeneration and myelin formation during the chronic recovery phase after stroke [6]. Repair-associated microglial states can support debris clearance, resolution of inflammation, extracellular matrix remodeling, and trophic support, thereby creating a permissive niche for OPC differentiation and remyelination [7]. In addition, emerging evidence indicates that microglia-derived extracellular vesicles (EVs) can directly contribute to post-stroke recovery [8]. This dynamic, context-dependent plasticity suggests that microglia are not simply indicators of injury severity but are active determinants of the repair environment [9]. Consequently, therapeutic strategies that shift microglial programs toward repair-permissive states may offer a more rational route to promote white matter restoration.

Accumulating evidence indicates that neurosteroids and their receptors act as important upstream regulators of microglial inflammatory programs [10]. In the CNS, steroids can be synthesized de novo and shape neuroinflammatory responses in a context- and cell type–dependent manner [10, 11]. Estrogens signal through ERα and ERβ (as well as membrane-associated receptors such as GPER) and have been reported to suppress microglial expression of pro-inflammatory mediators, including TNF, IL-6, IL-1β, and iNOS[12]. Mechanistically, ERβ signaling can engage transrepression and recruit corepressor complexes such as CtBP to dampen pro-inflammatory transcriptional programs, thereby constraining NF-κB-dependent responses in microglia [13]. Human Microglia Synthesize Neurosteroids to Cope with Rotenone-Induced Oxidative Stress. Notably, human microglia have also been reported to synthesize neurosteroids as an intrinsic mechanism to cope with oxidative stress [14]. Collectively, these findings support therapeutic interest in leveraging neurosteroid receptor pathways to fine-tune microglial activation states and create a repair-permissive environment for post-stroke white matter restoration.

Traditional Chinese medicine (TCM) formulas, with multi-component and multi-target characteristics, have attracted increasing interest as recovery-phase interventions for complex post-stroke pathophysiology [15, 16]. Danggui-Shaoyao-San (DSS), also known as the Decoction of Chinese Angelica and Peony, is a famous and classical traditional Chinese herbal formula. It has been historically used to treat gynecological disorders and chronic inflammatory conditions. This formula is composed of six raw herbs: Paeoniae Radix Alba (PRA), Atractylodes macrocephala Koidz. (AMK), Chuanxiong Rhizoma (CR), Angelicae Sinensis Radix (ASR), and Poria cocos (Schw.) Wolf (PCW) [17, 18]. In recent years, DSS has attracted attention for its potential neuroprotective and neurorestorative effects in neurological diseases, including ischemic stroke [19, 20]. Prior work suggests that DSS can inflammatory responses and influence microglial activation states in vitro [21]. In addition, we previously found that DSS promotes post-stroke neurological recovery by enhancing neurogenesis and angiogenesis [22]. Notably, our previous network pharmacology analysis of DSS for ischemic stroke showed that functional classification of drug–disease targets highlighted enrichment in "response to steroid hormone", and KEGG pathway enrichment implicated the estrogen signaling pathway, supporting the involvement of steroid hormone–related signaling in DSS actions [23]. However, whether DSS promotes long-term recovery by reshaping microglia-driven paracrine supports for oligodendroglia maturation and remyelination, and through which upstream signaling axis, remains unclear.

In this study, we investigated whether post-ischemic DSS supplementation improves long-term neurological recovery after transient middle cerebral artery occlusion (tMCAO), with a particular focus on white matter integrity and oligodendroglia regeneration. Based on the established role of microglia in shaping the lesion microenvironment, we further examined whether DSS alters post-stroke microglial polarization toward a reparative profile and whether DSS-related immune modulation is associated with enhanced myelin preservation and oligodendrocyte lineage progression. Finally, given the growing evidence that neurosteroid receptor pathways can control microglia-mediated inflammation, we considered neurosteroid signaling as a mechanistic axis potentially linking DSS treatment to microglial reprogramming and white matter repair.

MATERIALS AND METHODS

Animals

Male C57BL/6J mice (8–10 weeks, 22–25 g) were purchased from Beijing Vital River Laboratory Animal Technology Co., Ltd. (certification no. SCXK-2019-

0009) and housed in the SPF barrier facility of Capital Medical University (room temperature 22 ± 2 °C, 45–65 % humidity, 12-h light/dark cycle, lights on at 07:00) with ad libitum access to standard irradiated chow and autoclaved water. After a 7-day acclimation period, animals were randomly allocated to experimental groups. All surgical and experimental procedures were performed according to the NIH Guide for the Care and Use of Laboratory Animals. The study protocol was reviewed and approved by the Capital Medical University Animal Ethics Committee (approval no. AEEI-2024-310). Every effort was made to reduce the number of animals used and to minimize pain or distress.

Middle cerebral artery occlusion

Transient MCAO was performed under isoflurane anesthesia (4% induction, 1.5% maintenance) using the intraluminal filament method. A 6-0 silicone-coated nylon monofilament was introduced through the external carotid artery and advanced 9–10 mm to occlude the origin of the middle cerebral artery. After 45 min the filament was withdrawn for reperfusion [24]. Core temperature was maintained at 37 ± 0.5°C throughout surgery with a feedback-controlled heating pad. Cerebral blood flow (CBF) was monitored by laser-speckle contrast imaging (PeriCam PSI, Perimed) to confirm occlusion (>80% reduction) and adequate reperfusion (>90% recovery). Sham-operated animals underwent identical surgical exposure without filament insertion.

Drug administration

Danggui-Shaoyao-San (DSS, molecular weight 36–50 kDa; MP Biomedicals) was dissolved in sterile drinking water (5% w/v) and administered by oral gavage at 1,820 mg/kg (18.2 µl/g body weight) twice daily, starting 30 min after reperfusion and continuing until the experimental endpoint. The dosage was converted from the human dose recommended in the drug instruction manual based on body surface area. Vehicle-treated mice received sterile drinking water. BrdU (Sigma-Aldrich) was injected intraperitoneally at 50 mg/kg/daily for the periods indicated.

Behavioral testing

All tests were conducted by investigators blinded to treatment during the light phase and commenced 3 days before surgery for habituation.

Beam-walk: mice traversed a 1 m wooden beam (12 mm diameter) elevated 30 cm; scores (0–5) were assigned for foot-slip frequency and traversal time.

Wire-hang: latency to fall from an inverted 2-mm wire (maximum 150 s) was recorded in three consecutive trials.

Y-maze spontaneous alternation test: Short-term spatial working memory was evaluated using the Y-maze spontaneous alternation paradigm, following established procedures. The apparatus consisted of three identical arms (35 cm length × 5 cm width × 15 cm height) arranged symmetrically at 120° (Shanghai Xinruan Information Technology, Shanghai, China). Each mouse was placed at the central junction and allowed to freely explore the maze for 5 min. Arm entries were recorded, and a spontaneous alternation was scored when the animal entered all three arms consecutively (i.e., overlapping triplets of successive entries). The total number of arm entries and the number of alternations were counted. The alternation percentage was calculated as:

[(spontaneous alternations) / (total number of arm entries-2)] × 100% [25].

Morris water-maze: a 10-cm hidden platform was placed in the north-east quadrant of a 120-cm circular pool. Mice received four daily training trials (days 22–26 post-MCAO) with randomized start positions; escape latency was averaged per day. Probe trial (day 27) consisted of a 60-s free swim without platform; platform crossings and time in target quadrant were quantified via EthoVision XT (Noldus).

Two-dimensional laser speckle imaging

Regional cerebral blood flow (CBF) was monitored by the two-dimensional laser speckle imaging before ischemia and after the onset of ischemia (10 min after MCAO). We calculated the blood flow ratio of the two cerebral hemispheres (right/left), and at a ratio less than 20 %, the MCAO model was considered successful.

Immunofluorescence

Mice were anesthetized by intraperitoneal injection of 2% pentobarbital sodium (40 mg/kg) and transcardially perfused with 0.9% saline, followed by 4% paraformaldehyde (PFA) in PBS. Brains were collected, post-fixed overnight at 4 °C, cryoprotected in 30% sucrose, embedded, and cut into 15 µm coronal sections. Sections were blocked in 5% normal donkey serum containing 0.3% Triton X-100 for 1 h at room temperature and then incubated overnight at 4 °C with pairs of primary antibodies (Supplementary Table 1). After washing in PBS, sections were incubated with species-matched Alexa Fluor 488/555 secondary antibodies (1:300; Invitrogen) for 1 h at room temperature. Nuclei were counterstained with DAPI, and sections were mounted with Fluoromount-G. Images were acquired using a Leica

fluorescence microscope (20×/0.8 NA or 63×/1.4 NA objectives) with identical acquisition settings across groups. Image acquisition and quantitative analyses were performed by investigators blinded to group allocation.

Western blot assay

Cells were harvested on ice, washed with cold PBS, and lysed for protein extraction. Cell pellets were resuspended in RIPA buffer supplemented with protease and phosphatase inhibitors, and lysates were cleared by centrifugation. Protein concentrations were determined using a BCA assay. Equal amounts of protein were separated by SDS–PAGE and transferred to PVDF membranes. Membranes were blocked with 10% non-fat milk in TBST for 1 h at room temperature and incubated overnight at 4°C with primary antibodies (Supplementary Table 2). After three washes with TBST, membranes were incubated with appropriate HRP-conjugated secondary antibodies (1:3000, Zhongshan Golden Bridge) for 1 h at room temperature. Immunoreactive bands were visualized using enhanced chemiluminescence (Thermo Fisher Scientific) and quantified with ImageJ. Target protein signals were normalized to β-actin/GAPDH, and relative expression was calculated as the ratio of target band intensity to β-actin/GAPDH band intensity.

Transmission Electron microscopy

For transmission electron microscopy, mice were transcardially perfused with ice-cold saline followed by Servicebio G1102 fixative. The corpus callosum adjacent to the ischemic lesion was micro-dissected into 1 mm^3 blocks, post-fixed in fresh fixative, rinsed in 0.1 M PB (pH 7.4), and osmicated with 1% OsO4. After graded dehydration (30 – 100% ethanol and acetone), tissue was infiltrated with SPI-Pon 812 resin and polymerized at 60 ° C for 48 h. Semi-thin sections (1.5 µm) were toluidine-blue stained for light-microscopic targeting. Ultrathin sections (70 nm) were collected on 150-mesh formvar-coated copper grids, contrasted with 2 % uranyl acetate and 2.6 % lead citrate, and imaged in a TEM [26]. For each animal, at least 30 randomly selected axons were analyzed by blinded tracing of the axonal perimeter and the entire fiber perimeter. G-ratios were calculated as the ratio of the inner axon diameter to the total outer diameter (axon diameter plus total myelin sheath thickness).

DSS serum extraction

DSS serum was prepared following a previously described protocol [27] with minor modifications. Twenty Sprague–Dawley rats were randomly assigned to DSS and control groups. Rats in the DSS group received DSS at 1.26 g/kg by oral gavage twice daily for 7 days; controls received equivalent volumes of saline. One hour after the final dose, blood was collected from the abdominal aorta. Samples were left to clot for 2 h, centrifuged to obtain serum, and the serum was sterilized by passage through a 0.22 µm filter before use.

Cell culture and conditioned-medium generation

BV-2 murine microglia (BV-2, 20009P, Wuhan Servicebio) were cultured in complete medium (89% DMEM, 10% FBS, 1% penicillin–streptomycin) at 37°C under 5% CO_2. For experiments, cells were seeded at 2 × 10^5 cells/ml in 6-well plates or 1 × 10^6 cells/ml in 60 mm dishes, allowed to attach 4–6 h, and then changed to serum-free DMEM containing LPS (1 µg/ml, Sigma L4391), 5% DSS + 5% FBS, 10% NaCl, or fulvestrant (100 nM, MCE HY-13636, dissolved in 0.1% DMSO) for 24 h. After treatment, cells were harvested for RT-qPCR/Western blot, and the supernatants were collected, mixed 1:1 with differentiation medium (DMEM/0.5% FBS), and used immediately as conditioned medium (CM).

OLN93 rat oligodendrocyte progenitors (OLN93, 359390, BeNa Culture Collection) were maintained in DMEM supplemented with 10% FBS and 1% PS. Upon reaching 70–80 % confluence, cells were passaged with 0.25% trypsin, re-plated at 2 × 10^5 cells/ml in 6-well plates and switched to differentiation medium (DMEM/0.5% FBS). They were then cultured for 3 days with either PBS, PBS-CM, 5% DSS + 5% FBS, or 5% DSS + 5% FBS-CM. Cells and media were collected for subsequent RT-qPCR and Western blot analyses.

Cell viability analysis

The viability of BV2 cells was assessed using the Cell Counting Kit-8 (CCK-8), following previously described procedures [24]. The BV-2 cells were treated with FBS (DMEM + 10% FBS) and varying concentrations of DSS-serum (5% and 10%) for 24 h. Cell viability was subsequently measured using the CCK-8 methods.

RT-qPCR

Peri-infarct cortical-excluded brain tissue was micro-dissected from mice; BV-2 cells were serum-starved 4–6 h and then exposed for 24 h to LPS, 5% DSS + 5% FBS drug-containing serum, or the estrogen-receptor antagonist fulvestrant. OLN93 cells were differentiated for 3 days in either PBS or microglial conditioned medium (5% DSS + 5% FBS) or directly in PBS versus 5%DSS + 5% FBS drug serum. Total RNA was extracted with the

RNeasy Mini Kit (Vazyme), reverse-transcribed using the All-in-One RT kit (TransGen), and quantified on a Quantitect SYBR Green system (Cwbiotech) under the following cycling protocol: 95 °C 10 min; 40 cycles of 95°C 10 s, 60°C 30 s. Each sample was run in triplicate. mRNA levels of TNF-α, iNOS, IRF-4, IL-4, IL-1β, CD206, IRF-5, IL-10, Ptn and Timp1 were normalized to β-actin via the 2−ΔΔCT method; primers were synthesized by Sangon Biotech (Shanghai, China) and are listed in Supplementary Table 3.

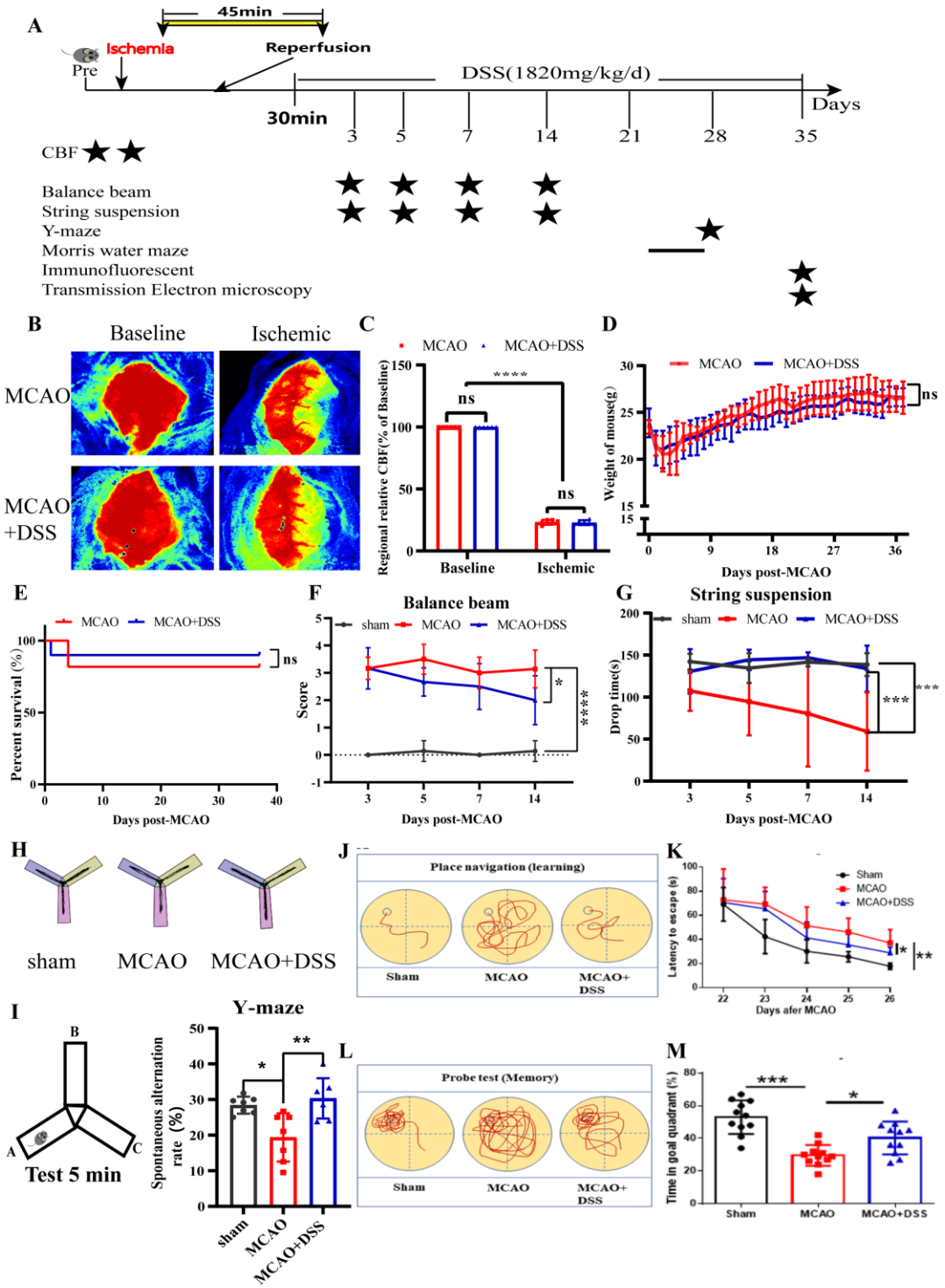

Figure 1. DSS promotes long-term functional recovery after transient focal cerebral ischemia. (A) Study design and behavioral testing schedule **(B)** Representative laser-speckle perfusion maps and **(C)** quantification of CBF during baseline and occlusion (n = 6), baseline CBF was set as 100%. **(D)** Body weight changes in both groups of mice (n = 10). (E) Kaplan–Meier survival to day 35 (MCAO, n = 10-12; MCAO + DSS, n = 10-11). **(F)** Beam-walk (n = 10) and (G) wire-hang tests (n = 10). **(H, I)** Y-maze spontaneous alternation and quantification (n = 6). **(J, K)** Morris water-maze acquisition and escape latency. **(L)** Representative probe-trial swim paths and (M) probe-trial measures of target preference (n = 10). Data are presented as mean ± SD. Statistical tests are indicated on the panels: two-way ANOVA with Tukey's post hoc test for longitudinal/behavioural measures, log-rank test for survival and one-way ANOVA followed by Tukey's multiple comparison test for other comparisons. ns: not significant; * $P < 0.05$, ** $P < 0.01$, *** $P < 0.001$, **** $P < 0.001$.

Quantification and statistics

Normality of data distribution was assessed using the Shapiro-Wilk test. For data that did not meet normality assumptions or for groups with sample sizes $N < 6$, non-parametric alternatives were used (Mann-Whitney U test for two-group comparisons; and Kruskal-Wallis test followed by Dunn's post hoc test with Bonferroni correction for multiple comparisons). For normally distributed data with appropriate sample sizes ($N \geqslant 6$), parametric tests were applied as follows: two-way repeated-measures ANOVA followed by Tukey's post hoc test for longitudinal behavioral tests (e.g., escape latency in the Morris water maze, with time as the within-subject factor and group as the between-subject factor) and OPC regeneration gene RT-qPCR tests; and one-way ANOVA followed by Tukey's multiple comparison test for comparisons among three or more groups. Correlations were assessed with Spearman's rank correlation for non-normal data or $N < 6$. Effect sizes were reported as partial eta-squared (η^2) for ANOVA. Statistical significance was set at $P < 0.05$. All statistical analyses were performed using GraphPad Prism version 9.0 (GraphPad Software, San Diego, CA, USA), and data collection and analyses were conducted by researchers blinded to experimental group allocation to ensure objectivity.

RESULTS

DSS mitigates neurological deficits after focal cerebral ischemia

To evaluate the impact of DSS on long-term outcome after experimental cerebral ischemia, mice were subjected to transient focal ischemia and treated with DSS or vehicle (Fig. 1A). Laser-speckle imaging confirmed comparable reductions in cortical cerebral blood flow during occlusion and similar reperfusion after filament withdrawal between groups (Fig. 1B, C). DSS did not significantly affect post-stroke body weight trajectories (Fig. 1D) or survival compared with vehicle controls (Fig. 1E).

Neurological performance was evaluated in four complementary behavioral paradigms. (Fig. 1F-M). Compared with vehicle-treated MCAO mice, DSS-treated animals showed improved performance in the beam-walk and wire-hang tasks, indicating better coordination and grip strength (Fig. 1F, G). In the Y-maze spontaneous alternation test (Fig. 1H), total arm entries were reduced in MCAO mice relative to sham-operated controls ($P<0.05$). However, DSS group showed a markedly increased spontaneous alternation rate ($P < 0.01$) (Fig. 1I). In the Morris water maze, DSS-treated mice learned the platform location more efficiently during acquisition and displayed better memory retention in the probe trial, as reflected by greater preference for the target location (Fig. 1J–M). Together, these data indicate that post-ischemic DSS administration enhances neurological functional recovery.

DSS promotes neurological recovery through preservation of white matter integrity

Because white-matter damage is a major determinant of long-term disability after stroke[28], we next examined myelin and axonal integrity in the ipsilateral corpus callosum and striatum (Fig. 2A). Immunofluorescence for myelin-basic protein (MBP) and neurofilament-200 (NF-200) at day 35 revealed marked loss of myelin in vehicle-treated mice (Fig. 2B); whereas DSS treatment largely preserved MBP signal in both regions in the corpus callosum ($P <0.05$; Fig. 2C) and the striatum ($P <0.05$; Fig. 2D) relative to vehicle.

At 35 days after surgery, transmission electron microscopy of the corpus callosum showed pronounced myelin abnormalities in the MCAO group, including myelin defects (blue arrows), whereas DSS-treated mice displayed relatively preserved myelin structure with remyelinated axons (red arrows) (Fig. 2E; insets show higher magnification).

We then quantified myelination using g-ratio analysis stratified by axon diameter (Fig. 2F). For axons with diameters of 0.4–0.8 μm, there was no significant difference between the MCAO and MCAO + DSS groups. In contrast, for axons with diameters > 0.8 μm, the DSS group exhibited a significantly lower g-ratio than the MCAO group, indicating thicker myelin and improved myelination. The scatter plot of individual g-ratios further

supported a downward shift in g-ratio values in DSS-treated mice, particularly among larger-caliber axons (Fig. 2G).

Finally, to examine the relationship between white-matter integrity and behavioral outcomes, we performed Pearson correlation analyses (n = 5). The MBP/NF200 ratio in both the corpus callosum and striatum was associated with behavioral performance, showing correlations with Y-maze spontaneous alternation (Fig. 2H, 2J) and Morris water-maze platform time (Fig. 2I, 2K). These correlations support a causal link between DSS-induced white-matter protection and improved cognitive outcome.

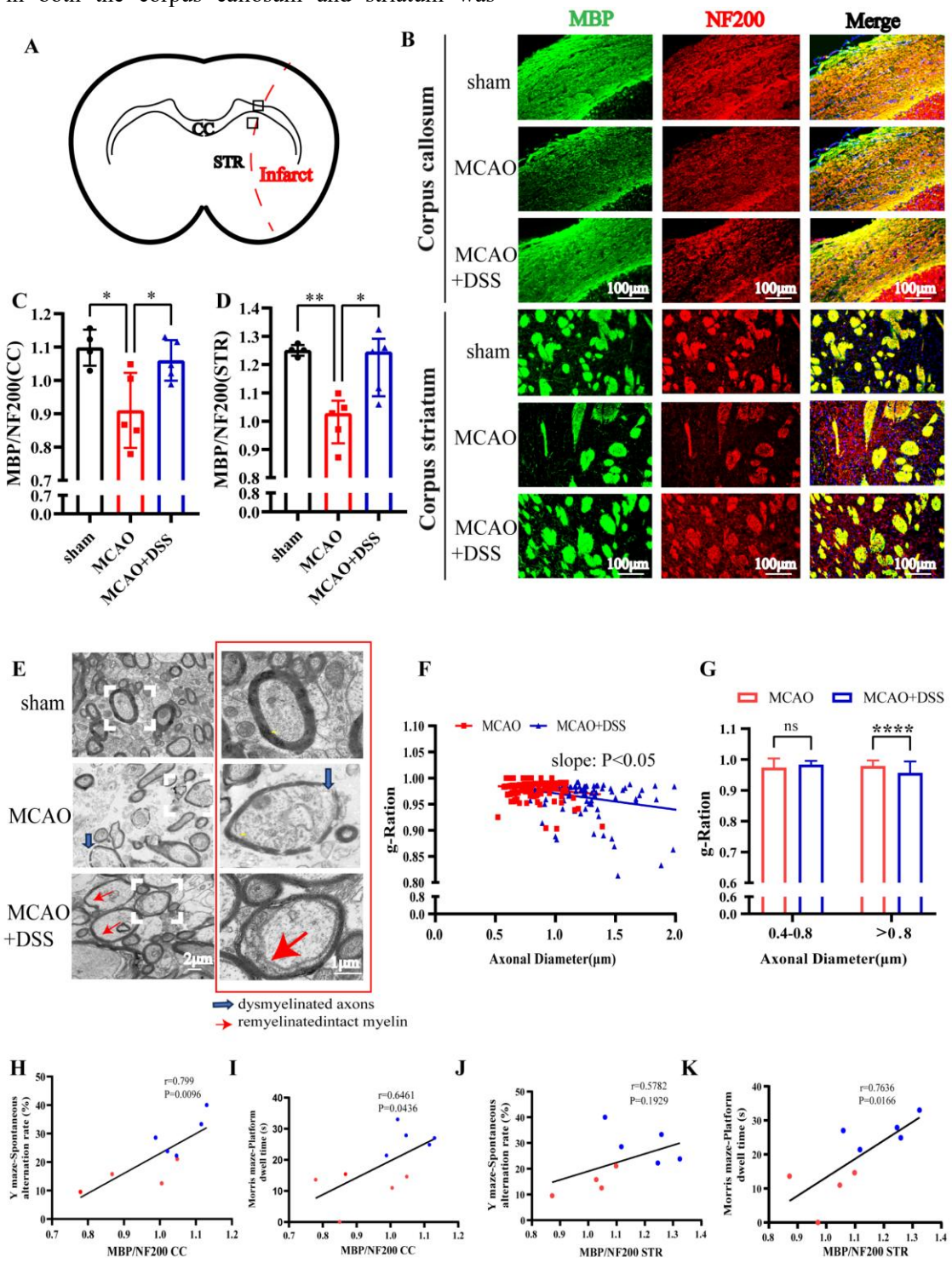

Figure 2. DSS preserves white-matter integrity after tMCAO. (A) Schematic of peri-infarct regions analyzed in corpus callosum (CC) and striatum (STR). **(B)** Representative images of myelin-basic protein (MBP, green) and neurofilament-200 (NF-200, red) at day 35, Scale bars: 100 µm. **(C, D)** Quantification of MBP/NF200 fluorescence intensity in CC and STR (n = 5). **(E)** Transmission-electron micrographs; blue arrows indicate dysmyelinated axons, red arrows indicate remyelinated/intact myelin. Insets show higher magnification. Scale bars, 2 µm (left) and 1 µm (right). **(F)** G-ratio frequency distribution stratified by axon diameter and **(G)** cumulative probability plot of individual g-ratios, where each data point represents the average g-ratio per axon (n = 6 mice, ~350 axons per mouse). **(H)** Correlation between corpus callosum MBP/NF-200 ratio and Y-maze alternation (n = 4). (I) Correlation between corpus callosum MBP/NF-200 ratio and Morris water-maze time in target quadrant (n = 5). **(J)** Correlation between striatal MBP/NF-200 ratio and Y-maze alternation (n = 5). **(K)** Correlation between striatal MBP/NF-200 ratio and Morris water-maze time in target quadrant (n = 5). Data are presented as median with interquartile range (IQR) for fluorescence analyses. Kruskal-Wallis test followed by Dunn's post hoc test with Bonferroni correction was used for multiple comparisons. For transmission electron microscopy data, data are presented as mean ± SD and were analyzed by two-way ANOVA with Tukey's post hoc test. Spearman's rank correlation was used to analyze the correlation. ns: not significant; * $P < 0.05$, ** $P < 0.01$, **** $P < 0.0001$.

DSS increases mature oligodendrocyte density and promotes oligodendrocyte precursor differentiation

Because oligodendrocytes are the myelin-forming cells in white matter and their loss or failed maturation after ischemia underlies demyelination and impaired axonal conduction [29], we examined the oligodendroglial lineage to determine whether DSS preserves myelin by affecting oligodendrocyte precursor cells (OPCs) proliferation, survival, or maturation. DSS significantly increased $CNPase^+$ mature oligodendrocyte density in peri-infarct white-matter regions compared with the MCAO group (Fig. 3A, B). Pearson correlation analysis showed that $CNPase^+$ cell number correlated positively with Y-maze alternation ($r = 0.76$, $P = 0.048$) and negatively with Morris water-maze escape latency ($r = -0.91$, $P = 0.0008$) (Fig. 3C, D), indicating that preservation of mature oligodendrocytes is associated with improved cognitive and spatial performance.

To determine whether DSS targets OPCs, we assessed OPC proliferation and differentiation. At day 7, the density of proliferating OPCs ($PDGFR\alpha^+BrdU^+$) did not differ between DSS and vehicle groups (Fig. 3F,G), indicating no pro-proliferative effect. By contrast, the number of newly generated $CNPase^+BrdU^+$ oligodendrocytes was higher in DSS-treated brains ($P < 0.001$; Fig. 3H, I). Collectively, these data demonstrate that DSS does not expand the OPC pool but instead accelerates the differentiation of OPCs into mature, myelin-forming oligodendrocytes, thereby contributing to white-matter repair and functional recovery.

DSS restrains pro inflammatory microglia and expands the restorative population after MCAO

To determine whether the functional and white-matter benefits of DSS were accompanied by modulation of post-ischemic neuro-inflammation, we examined microglial polarization in the striatum and corpus callosum at 3, 7 and 14 days after reperfusion. Immunofluorescence labelling for the pan-microglial marker Iba1 together with CD16/32 (pro-inflammatory microglia phenotype) revealed a robust rise in pro-inflammatory microglia in vehicle-treated mice that was apparent by day 3 and remained elevated through day 14 (Fig. 4A–F). DSS administration almost significantly reduced the number of Iba1+CD16/32+ cells in both the striatum and corpus callosum at every time point examined (Fig. 4G, H). RT–qPCR analysis of infarcted brain tissue collected at 3, 7 and 14 days after tMCAO further supported the immunohistochemical findings. Transcripts encoding the pro-inflammatory-associated molecules iNOS, IRF-4 and IL-6 were markedly upregulated in vehicle-treated mice and remained elevated through day 14, whereas DSS treatment significantly attenuated their expression at the acute phase and promoted subsequent normalisation (Fig. 4I-K).

Conversely, staining for the restorative marker CD206 showed an expansion of restoration-oriented microglia in DSS-treated animals. Quantification of $Iba1^+CD206^+$ signal demonstrated increased restorative microglia in the peri-infarct region and corpus callosum at later time points (Fig. 5A–H). Consistent with these observations, RT–qPCR of infarcted tissue collected at 3, 7 and 14 days showed higher expression of the restorative markers CD206, IRF-5 and IL-10 in DSS group, particularly at days 7 and 14 (Fig. 5J-M). Collectively, these data indicate that DSS suppresses post-ischemic pro-inflammatory microglial activation while promoting a sustained, tissue-restorative microglial milieu after experimental stroke.

DSS containing serum shifts BV2 microglia toward a restorative phenotype

To determine whether DSS-containing serum both dampens inflammatory activation and enhances pro-restorative features in microglia in vitro, BV2 microglia were exposed to rat-derived DSS-containing serum or control serum and then treated with LPS. CCK-8 viability assay in BV2 cells (n = 4) showed no significant cytotoxicity for either 10% DSS serum or 5% DSS + 5%

FBS versus complete-medium control; because 5% DSS + 5% FBS produced the highest mean viability, this condition was selected for subsequent in vitro experiments (Fig. 6A, B).

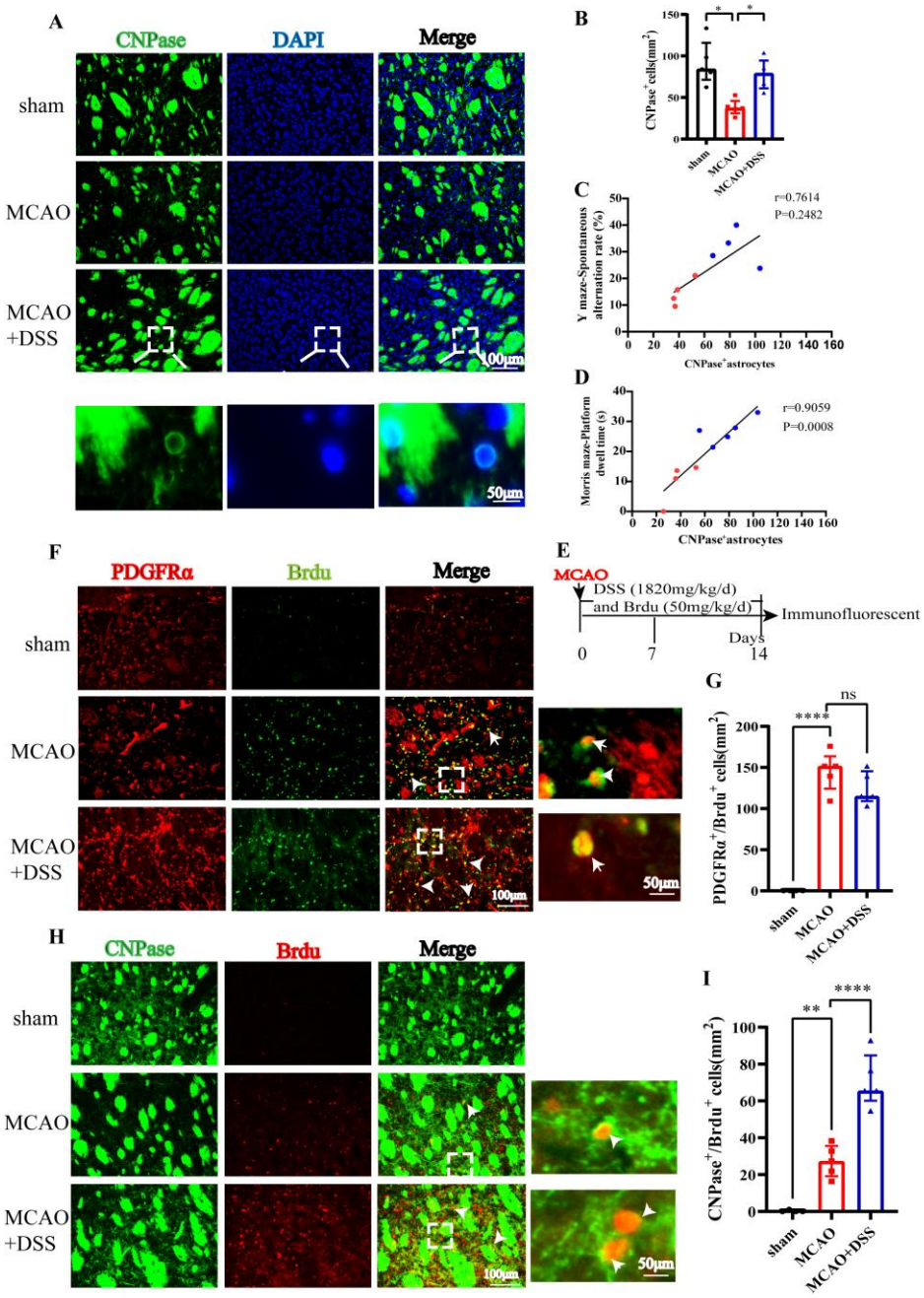

Figure 3. DSS-induced functional recovery is coupled to preservation of mature oligodendrocytes and accelerated OPC differentiation after tMCAO. **(A)** Representative fluorescence microscopy images of CNPase$^+$ mature oligodendrocytes in peri-infarct white-matter at day 35; inset shows high-magnification detail. **(B)** Quantification of CNPase$^+$ cell density (n = 4). **(C, D)** Pearson correlations between CNPase$^+$ density and Y-maze alternation ratio (C) (n = 4) or water-maze time in target quadrant (D) (n = 4-5). **(E)** Timeline for experimental. **(F)** Representative fluorescence microscopy images of PDGFRα$^+$BrdU$^+$ OPCs at day 7, arrowhead: PDGFRα$^+$BrdU$^+$ expression. **(G)** Quantification of PDGFRα$^+$BrdU$^+$ OPCs (n = 5). **(H)** Representative fluorescence microscopy images of CNPase$^+$BrdU$^+$ newly generated oligodendrocytes at day 14, arrowhead: CNPase$^+$BrdU$^+$ expression. **(I)** Quantification of CNPase$^+$BrdU$^+$ cells (n = 5). Data are presented as median with IQR. Kruskal-Wallis test followed by Dunn's post hoc test with Bonferroni correction for multiple comparisons. Spearman's rank correlation. ns: not significant; * P < 0.05, **P < 0.01, ****P < 0.0001. Scale bars: 100 μm (low magnification); 50 μm (insets).

Schematic of the in vitro treatment paradigm was shown in Fig. 6C. LPS robustly induced pro-inflammatory cytokine transcripts, whereas DSS-containing serum significantly reduced the LPS-driven upregulation of TNF-α and IL-1β (n =4-5; Fig. 6D, E). Consistently, Western blotting showed that DSS-containing serum decreased iNOS protein abundance relative to LPS controls (n = 4; Fig. 6H, I). Together, these data indicate that DSS-containing serum redused LPS-induced inflammatory activation in BV2 microglia in vitro.

In parallel, we assessed restoration-associated reparative markers. DSS-containing serum increased CD206 and IL-10 mRNA levels (n = 4-5; Fig. 6F, G) and elevated the Arg1 protein level by Western blotting (n =

3-4; Fig. 6H, J), supporting a shift toward a restorative microglia phenotype.

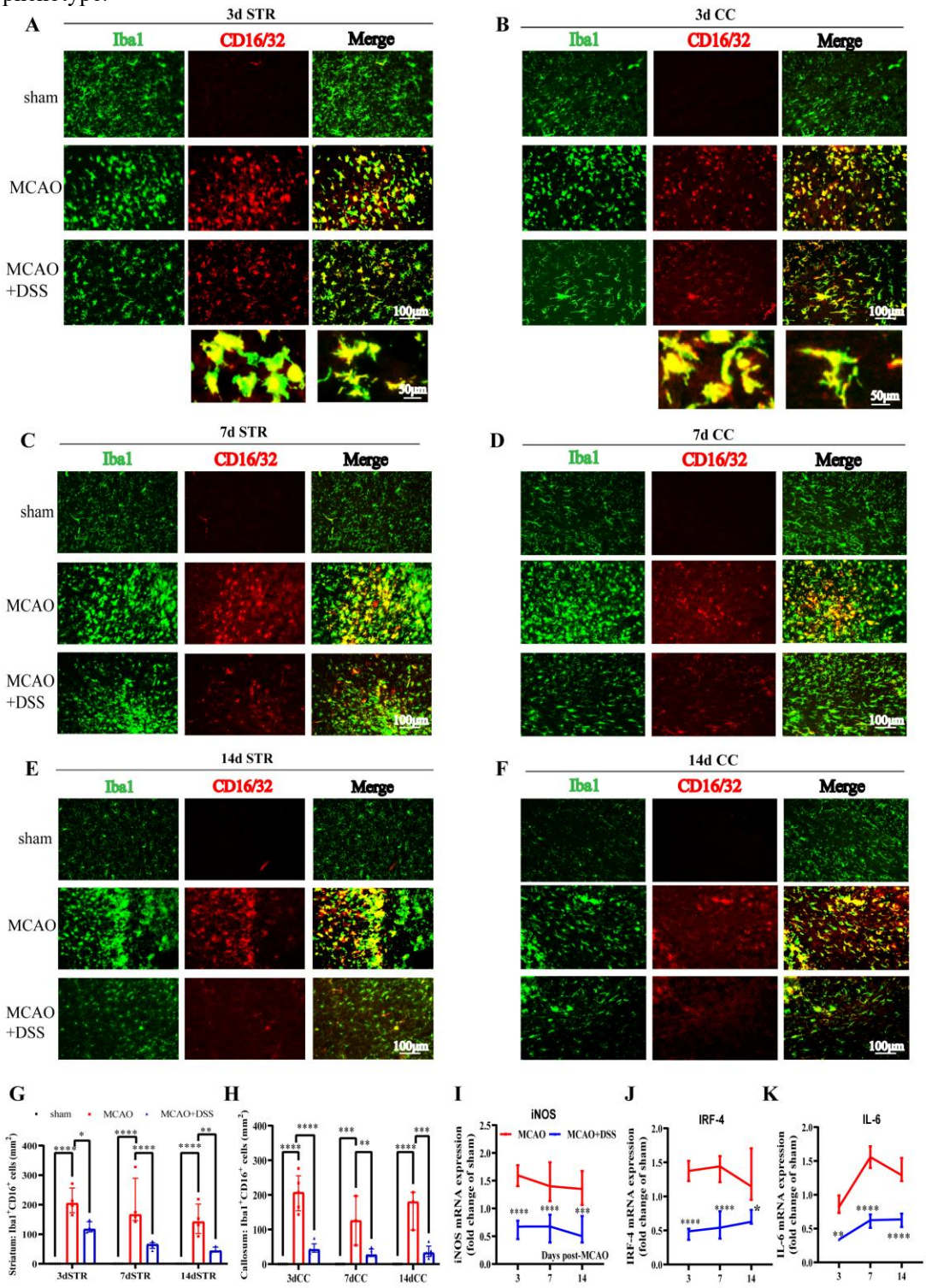

Figure 4. DSS suppresses the pro-inflammatory microglia response after tMCAO. (A–F) Representative images of Iba1^{+}CD16/32^{+} cells at 3, 7 and 14 days post-reperfusion in the striatum (STR) and corpus callosum (CC), higher magnification insets are shown below B and C panel. **(G, H)** Group data showing the number of Iba1^{+}CD16/32^{+} cells per mm^2 in the STR (G) (n = 4) and CC (H) (n = 3-4). **(I-K)** RT-qPCR analysis of pro-inflammatory genes (iNOS, IRF-4, IL-6) in infarcted tissue (n = 4). Data are normalized to sham-operated controls and presented as median with IQR. Kruskal-Wallis test followed by Dunn's post hoc test with Bonferroni correction was used for multiple

comparisons among three groups; for two-group comparisons, Mann-Whitney U test was used. * P < 0.05, **P < 0.01, ***P < 0.001, **** P < 0.0001. Scale bars: 100 μm (low magnification); 50 μm (insets).

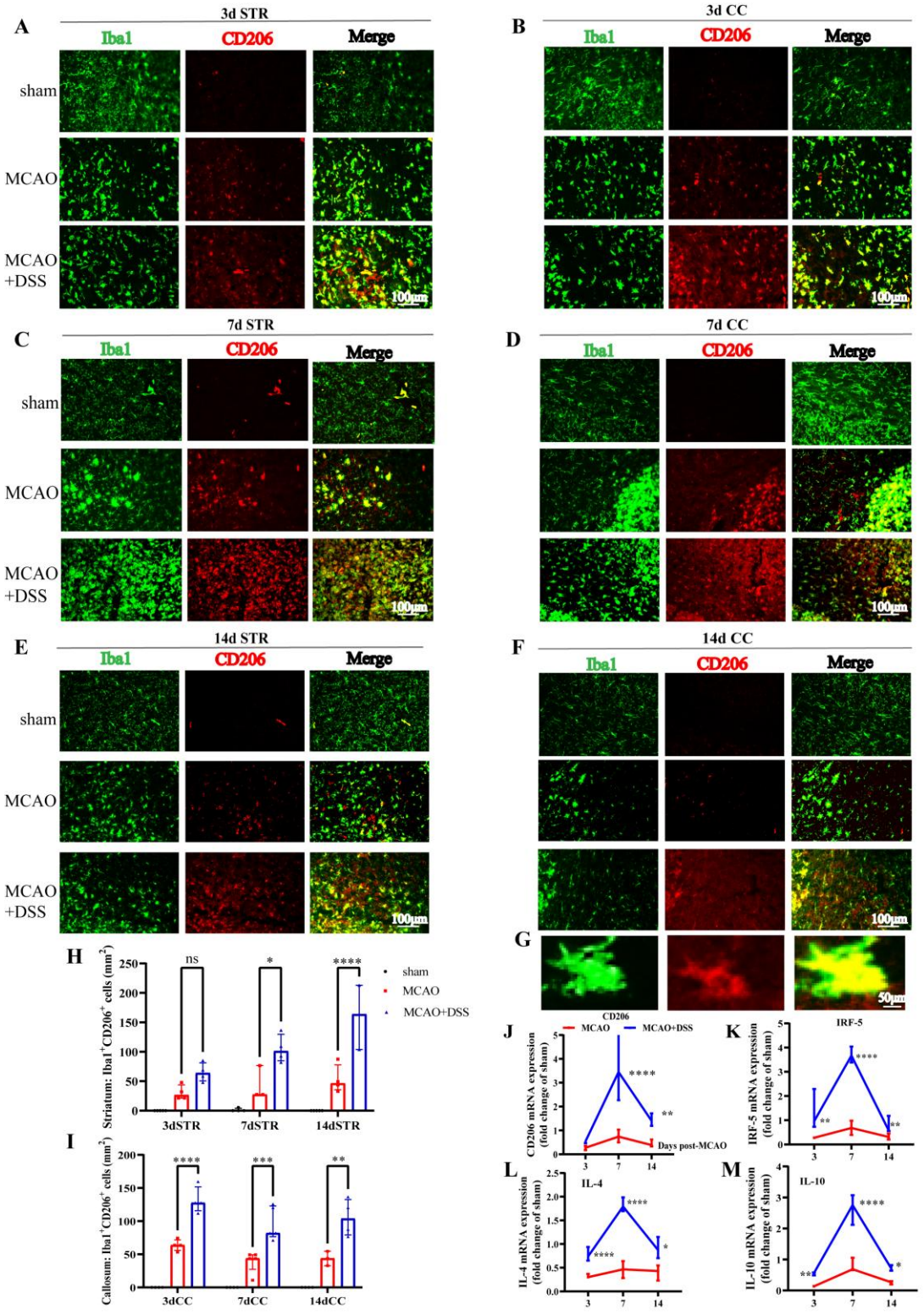

Figure 5. DSS expands the restorative microglia after tMCAO. (A–F) Representative images of Iba1$^+$CD206$^+$ cells at 3, 7 and 14 days post-reperfusion in the striatum (STR) and corpus callosum (CC). **(G)** Higher magnification insets. **(H, I)** Group data showing the number of Iba1$^+$CD206$^+$ cells per mm^2 in the STR (H) (n = 3-4) and CC (I) (n = 3-4). (J-M) Expression of repair-associated genes (CD206, IRF-5, IL-10, IL-4, respectively) (n = 4). Data are

normalized to sham-operated controls and presented as median with IQR. For multiple comparisons among three groups, Kruskal-Wallis test followed by Dunn's post hoc test with Bonferroni correction was used or Mann-Whitney U test was used for two-group comparisons. ns: not significant; *P < 0.05, **P < 0.01, ***P < 0.001, **** P < 0.0001. Scale bars: 100 μm (low magnification); 50 μm (insets).

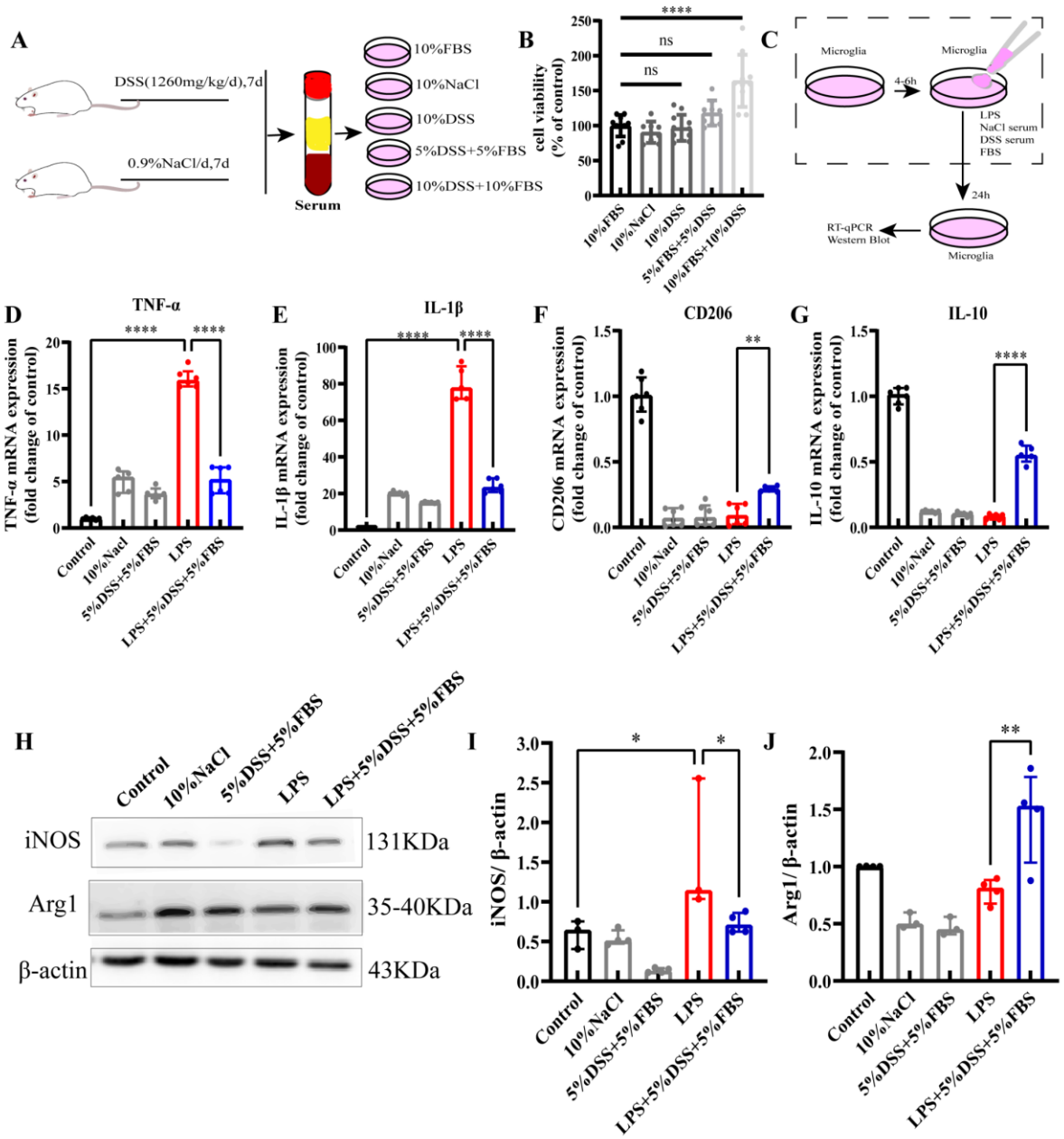

Figure 6. DSS-containing serum attenuates LPS-induced inflammatory activation in BV2 microglia in vitro. (A) Workflow for generating DSS-containing serum and control serum and applying them to BV2 cells. **(B)** CCK-8 cell viability across serum conditions used to select a non-toxic regimen (n = 6). **(C)** Experimental timeline for BV2 treatment and downstream assays. **(D-G)** RT-qPCR analysis of pro-inflammatory microglia markers TNF-α (D) and IL-1β (E), and restorative microglia markers CD206 (F) and IL-10 (G) (n = 4-5). **(H)** Representative Western blots of iNOS and Arg1 with β-actin as a loading control. **(I-J)** Densitometric quantification of iNOS (I) and Arg1 (J) normalized to β-actin (n = 3-4). Data are presented as mean ± SD for CCK-8 data analyzed by one-way ANOVA with Tukey's test, or median with IQR for all other data analyzed by Kruskal-Wallis test with Dunn's post hoc test. ns: not significant; *P < 0.05, **P < 0.01, ****P < 0.0001. DSS + FBS: serum from animals treated with DSS (medicated serum), supplemented with fetal bovine serum.

DSS treated microglial conditioned medium drives oligodendroglial differentiation in OLN93 cells

Given our in vivo findings implicating microglia in white-matter repair, we determine whether microglia-derived paracrine cues promote oligodendroglia differentiation. We first assessed the mature oligodendrocyte marker CNPase. In the microglial CM condition, OLN93 cells exposed to CM from DSS-treated microglia (5% DSS + 5%FBS CM) showed a significant increase in CNPase expression compared with control CM (Con CM) (n = 4-5; Fig. 7B, C). By contrast, in the direct effect condition (without microglial CM), direct DSS treatment (5% DSS + 5% FBS) did not significantly change CNPase expression compared to PBS control (Fig. 7B, C). Notably, in the Con CM group, CNPase levels were not different from baseline (Fig. 7C).

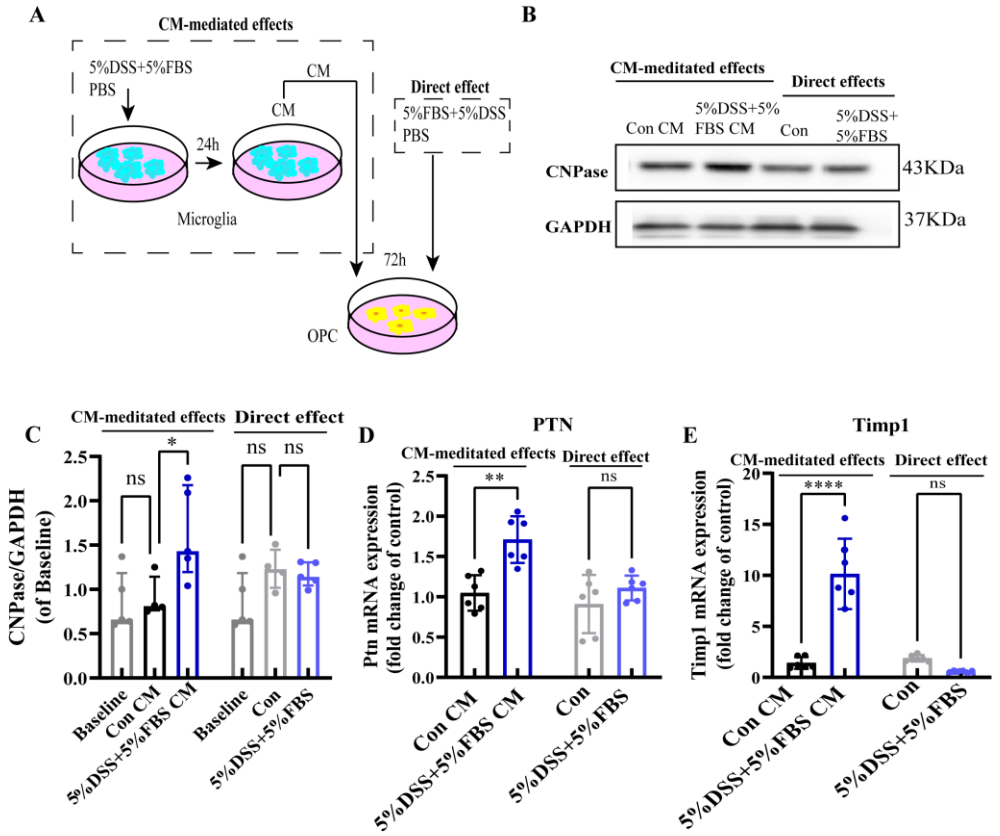

Figure 7. Conditioned medium from DSS-treated BV2 microglia promotes oligodendroglial repair-associated signals in OLN93 OPCs. (A) Schematic of BV2 treatment, CM collection, and OLN93 exposure (CM arm) alongside direct-treatment controls. **(B)** Representative Western blot for CNPase with GAPDH loading control. **(C)** Densitometric quantification of CNPase/GAPDH, expressed relative to baseline (n = 4-5). **(D–E)** RT-qPCR of Ptn and Timp1 in OLN93 cells following direct treatment (ns) or CM exposure (n = 6). Data are presented as median with IQR for western blot data analyzed by Kruskal-Wallis test followed by Dunn's post hoc test with Bonferroni correction or mean ± SD for RT-qPCR data analyzed by two-way ANOVA followed by Tukey's test. ns: not significant; *P < 0.05, **P < 0.01, ***P < 0.001.

We next examined whether DSS-modified microglial CM also induces expression of pro-regenerative factors in OLN93 cells. RT-qPCR analysis showed that, under the microglial CM condition, CM derived from DSS-treated microglia significantly increased expression of Ptn and Timp1 compared with control CM (Fig. 7D, E). In contrast, direct DSS treatment of OLN93 cells (without CM) did not significantly alter Ptn or Timp1 expression (Fig. 7D, E), indicating that these effects are primarily mediated by microglia-derived secreted cues rather than direct DSS action on OLN93 cells. Together, these results suggest that DSS reprograms microglial paracrine to support oligodendroglia differentiation and to upregulate regenerative gene expression.

DSS modulates microglial polarization *via* the neurosteroid receptor pathway

Our previous network pharmacology analysis predicted that DSS may regulate steroid hormone receptor–related

signaling [23]. Given evidence that neurosteroid receptors, particularly estrogen receptors (ERs), shape microglial activation and polarization, we next examined whether DSS engages ER signaling after ischemic stroke. Double immunofluorescence staining in peri-infarct white matter at day 3 after reperfusion showed increased ERα and ERβ expression in microglia in DSS-treated mice compared with vehicle controls, as indicated by a higher density of Iba1$^+$ERα$^+$ and Iba1$^+$ERβ$^+$ cells (Fig. 8A–C).

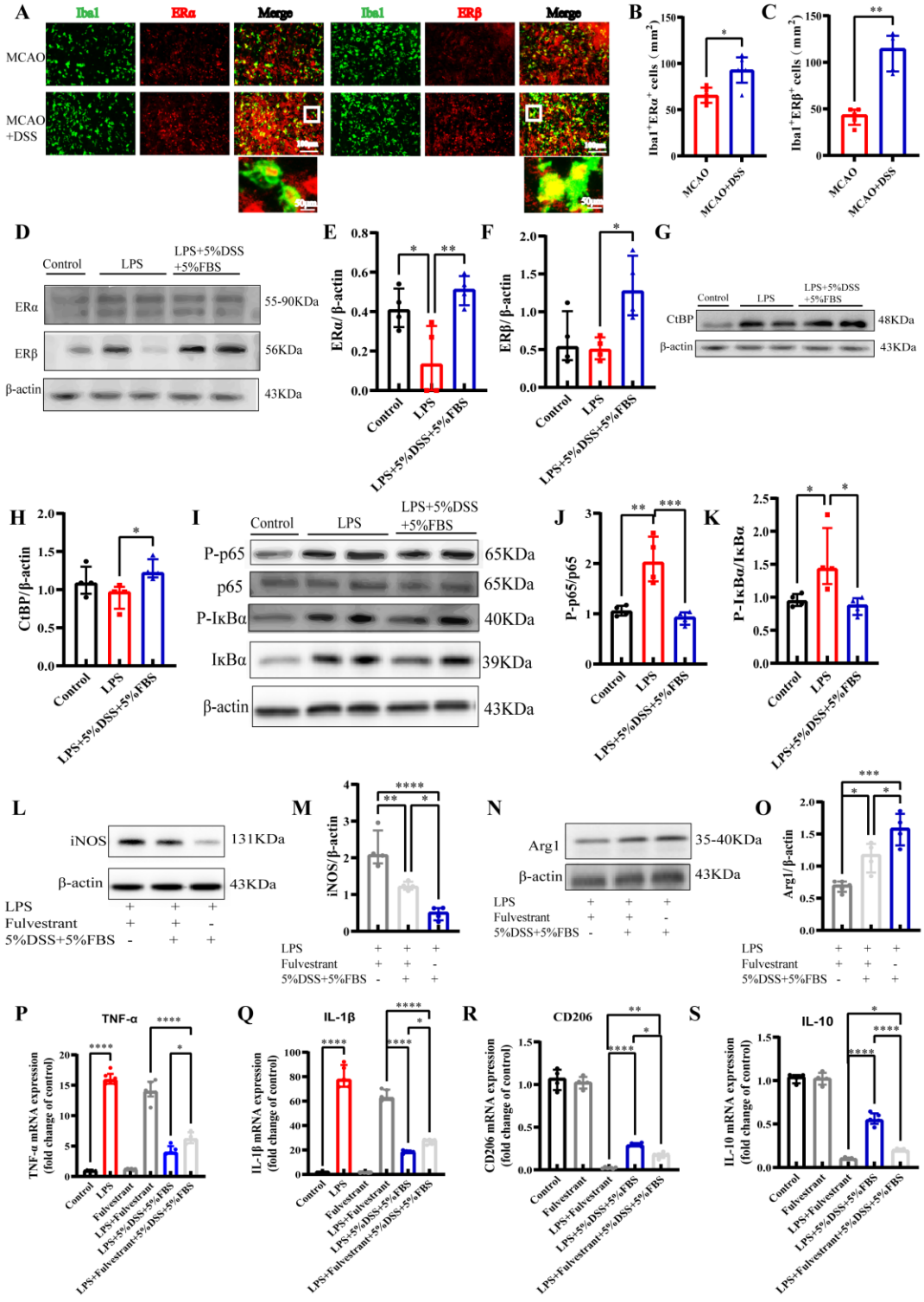

Figure 8. DSS modulates microglial polarization via the neurosteroid receptor pathway. (A) Representative immunofluorescence images and quantification of ERα and ERβ expression in peri-infarct white matter from the MCAO and MCAO + DSS groups at day 3 post-reperfusion. **(B)** Group data (n = 4 mice per group) showing the number of $Iba1^+ER\alpha^+$ cells per mm^2. **(C)** Group data (n = 4 mice per group) showing the number of $Iba1^+ER\beta^+$ cells per mm^2. **(D)** Representative Western blot images of ERα and ERβ in BV2 cells across treatment groups. **(E-F)** Quantification of relative ERα (E) and ERβ (F) protein levels, normalized to β-actin (n = 4). **(G)** Representative Western blot image of CtBP. **(H)** Quantification of relative CtBP protein level (n = 3-4). (I) Representative Western blot images of p-NF-κB p65, NF-κB p65, p-IκBα, and IκBα, normalized to the corresponding total protein. **(J-K)** Quantification of p-NF-κB p65/NF-κB p65 (J) and p-IκBα/IκBα (K) ratios (n = 4). **(L)** Representative Western blot image of iNOS. (M) Quantification of relative iNOS protein level (n = 4). **(N)** Representative Western blot image of Arg1. (O) Quantification of relative Arg1 protein level (n = 4). **(P–Q)** RT-qPCR analysis of TNF-α and IL-1β mRNA levels (n = 5). **(R–S)** RT-qPCR analysis of CD206 and IL-10 mRNA levels (n = 5). Data are presented as median with IQR. Mann-Whitney U test was used for two-group comparisons, and Kruskal-Wallis test followed by Dunn's post hoc test was used for multiple comparisons. *P < 0.05, **P < 0.01, ***P < 0.001, ****P < 0.0001. Scale bars: 100 μm (low magnification); 50 μm (insets).

Consistent with the in vivo observations, Western blot analysis in BV2 microglia further demonstrated that DSS treatment increased ERα and ERβ protein levels under inflammatory stimulation (Fig. 8D–F), suggesting enhanced neurosteroid receptor signaling. In parallel, Western blot analysis showed that DSS increased the expression of C-terminal binding protein (CtBP), an ER-interacting transcriptional corepressor implicated in repression of pro-inflammatory gene programs (Fig. 8G, H). Because ER signaling can antagonize NF-κB-dependent inflammatory transcription [10], we next assessed NF-κB pathway activation. Western blot analysis further revealed that DSS markedly reduced phosphorylation of NF-κB p65 and IκBα (Fig. 8I-K), indicating suppression of NF-κB signaling.

To functionally validate the involvement of ER signaling, BV2 microglia were co-treated with DSS-containing serum in the presence or absence of fulvestrant, a selective ER antagonist [30]. Western blotting showed that DSS-induced suppression of iNOS protein was partially reversed by fulvestrant (Fig. 8L, M), while the DSS-driven increase in Arg1 protein was attenuated upon ER blockade (Fig. 8N, O). Consistently, RT-qPCR analysis demonstrated that fulvestrant mitigated the effects of DSS on microglial polarization-related transcripts, restoring the expression of the pro-inflammatory cytokines TNF-α and IL-1β and reducing the DSS-induced upregulation of the restoration-associated markers CD206 and IL-10 (Fig. 8P-S).

DISCUSSION

Post-stroke disability is increasingly recognized to arise not only from irreversible neuronal loss but also from delayed secondary injury processes that impair white matter integrity and limit endogenous remyelination [31]. In this study, we demonstrate that delayed administration of Danggui-Shaoyao-San (DSS), initiated 30 minutes after reperfusion and maintained throughout the recovery phase, improves long-term neurological outcomes after transient focal cerebral ischemia. These functional benefits are accompanied by preserved myelin–axon coupling and improved myelin ultrastructure in peri-infarct white matter, together with enhanced progression of the oligodendrocyte lineage toward a mature, myelin-forming state. Molecular mechanistically, our data support a recovery-oriented model in which DSS enhances microglial estrogen receptor (ERα/ERβ) signaling, increases the ER-associated corepressor CtBP, and dampens NF-κB activation, thereby shifting microglia away from a pro-inflammatory program toward a more restorative phenotype that creates a permissive milieu for oligodendroglial differentiation and remyelination (Fig. 9).

White matter, composed mainly of myelinated fibers and glial cells, is essential for long-range neural communication and is frequently involved in cerebral infarction [32]. Because white matter integrity strongly constrains neurological recovery, promoting white matter repair has become an important strategy for improving long-term post-stroke outcomes [33]. Remyelination is a central component of white matter restoration and is driven by the differentiation and maturation of oligodendrocyte lineage cells; however, this endogenous program is often insufficient after stroke. After stroke, oligodendrocytes can be replenished from OPCs via proliferation, migration, and differentiation; however, differentiation is often limited, making the promotion of oligodendrocyte maturation and remyelination a key route to enhance white matter repair [34]. Currently, no approved drugs or targeted therapies exist for these conditions. In the study, we showed that DSS treatment was associated with improved myelin integrity and a more mature, myelin-forming oligodendrocyte lineage profile, and these changes correlated with better behavioral performance. Importantly, some studies have attributed post-stroke white matter improvement mainly to expanded OPC pools or enhanced oligodendrocyte survival [34, 35], In our study, we did not detect a major increase in OPC proliferation. We also did not observe a

clear anti-apoptotic effect in the oligodendrocyte lineage. These findings instead point to accelerated lineage progression as a likely driver of remyelination. This pattern is consistent with the view that, after stroke, the principal bottleneck for endogenous remyelination often lies in inefficient OPC differentiation/maturation [36, 37]. Together, these findings suggest that DSS may engage maturation-permissive mechanisms to overcome the post-stroke differentiation block, reinforcing white matter remodeling as a therapeutically actionable target in the recovery window.

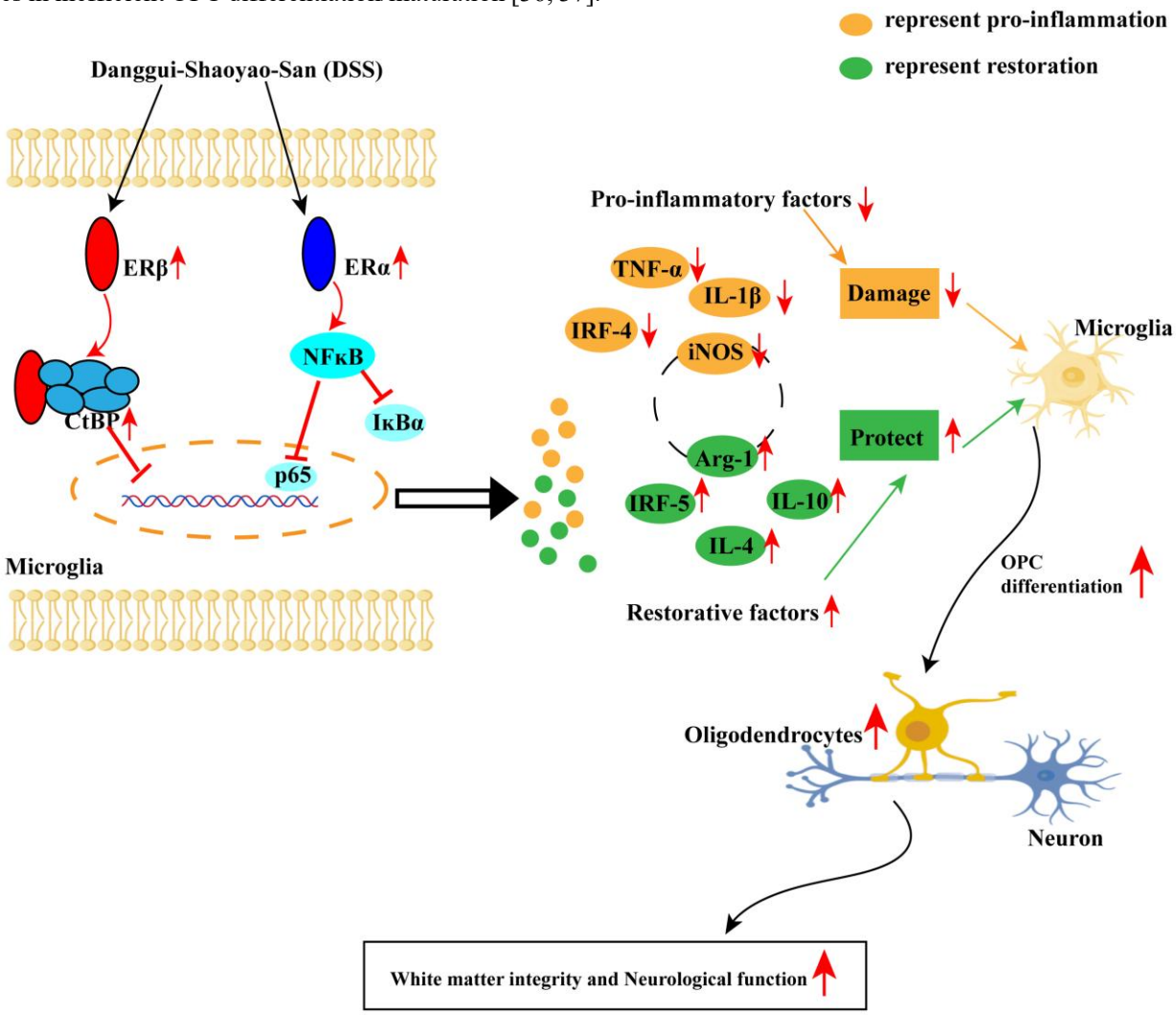

Figure 9. Proposed molecular mechanism of DSS promoting microglial reprogramming and remyelination in a mouse model of ischemic stroke. DSS administered after ischemic stroke activates estrogen receptor signaling (ERα/ERβ) in microglia, increasing CtBP and suppressing NF-κB activation (reduced p-IκBα and p-p65). This shifts microglial polarization away from a pro-inflammatory phenotype (↓ iNOS, TNF-α, IL-1β, IRF-4) toward a reparative/pro-resolving phenotype (↑ Arg1, CD206, IL-10, IRF-5). The DSS-reprogrammed microglial secretome then promotes OPC differentiation into mature oligodendrocytes, enhancing remyelination and white-matter integrity, which ultimately improves neurological function after tMCAO.

Existing evidence also supports a recovery-oriented therapeutic profile of DSS. Clinically, DSS added to conventional pharmacotherapy has been reported to improve neurological function, and combining DSS with rehabilitation training further enhances motor function and activities of daily living [38]. Studies have also suggested that DSS improves microcirculation/ hemorheological indices in cerebrovascular disorders, including reduced blood viscosity and improved erythrocyte deformability, alongside attenuation of oxidative stress–related markers [39]. Moreover, Zhu et al. reported that argatroban plus DSS reduced neurological deficit scores and improved hemorheological parameters compared with regimens without DSS [40]. Complementing these clinical observations, our previous animal work showed that DSS

promotes post-stroke angiogenesis [22]. Taken together, the results are consistent with DSS facilitating post-stroke functional recovery via multi-target regulation, and our data highlight white matter repair as a prominent correlate of the behavioral benefits.

A plausible mechanistic explanation for the chronic white matter benefits of DSS is that it redirects the post-ischemic microglial trajectory toward a repair-permissive program. Accumulating evidence indicates that persistently pro-inflammatory microglial activation impedes oligodendrocyte lineage progression, exacerbates demyelination and axon – myelin uncoupling, and thereby worsens neurological outcome [41]. In models of traumatic brain injury, suppressing pro-inflammatory microglial activation alleviates inflammatory injury and mitigates myelin loss [42], and in ischemic stroke, abnormal microglial activation amplifies neuroinflammation and increases white matter damage [43]. Conversely, restoration-associated microglial states support remyelination by promoting debris clearance, extracellular matrix remodeling, and trophic support [43]. Augmenting reparative microglial activity upregulates oligodendrogenic and pro-remyelinating factors (e.g., Tgm2, Vegfa, Timp1, FGF1, Ptn) to promote oligodendrocyte regeneration and myelin formation during chronic recovery [6]. Mechanistically, these effects are consistent with microglia-oligodendroglia crosstalk. In this framework, microglia-secreted cues regulate OPC lineage progression and maturation. Reparative microglia – derived extracellular vesicles can restore reparative function [44]. Microglia-derived extracellular vesicles can also enhance oligodendrocyte maturation [45]. Our results showed that DSS shifted microglial polarization toward a restoration-associated profile in vivo, in parallel with improved white matter indices. Consistent with an indirect paracrine mechanism, conditioned medium from DSS-treated BV2 microglia induced pro-differentiation and repair-associated signatures in OPCs. By contrast, direct exposure of oligodendroglia cells to DSS-containing serum did not. Collectively, our results support a model in which DSS promotes chronic white matter repair. DSS appears to reprogram microglial polarization and reshape the microglial secretome. These changes favor OPC-to-oligodendrocyte maturation and remyelination. Thus, reparative microglial activation may represent a therapeutically relevant target in ischemic stroke.

Our prior network-pharmacology analysis suggested that DSS may modulate steroid hormone–related pathways and ER signaling [23]. This observation aligns with a well-established body of evidence indicating that steroid hormones regulate multiple key functions of the central nervous system [46]. Peripheral steroid hormones (from the adrenal glands, gonads, and placenta) can cross the blood–brain barrier and act within the CNS as neuroactive steroids [10]. Prior studies indicate that steroid hormone receptors expressed in microglia—particularly estrogen receptors (ERs)—play an important role in shaping inflammatory versus reparative programs [47, 48]. In experimental autoimmune demyelination, ERβ has been shown to interact with the CtBP corepressor complex and to be recruited to AP-1–dependent promoters, resulting in the suppression of pro-inflammatory mediator transcription [13]. In models of traumatic brain injury and demyelinating disease, pharmacological ligands of ERα/ERβ increase receptor activity and reduce microglial expression of IL-6, IL-1β, iNOS, and COX2, conferring neuroprotection. Formononetin inhibits neuroinflammation and increases estrogen receptor beta (ERβ) protein expression in BV2 microglia [49]. Collectively, these observations support the view that ER-mediated transcriptional regulation represents an upstream control point that restrains myeloid inflammatory programs while facilitating inflammation resolution and tissue repair.

Against this background, we evaluated the effects of DSS on the microglial ER axis in both in vivo and in vitro settings. Integrating our results, DSS-induced microglial phenotypic remodeling appears to be driven, at least in part, by ER-dependent receptor–transcription coupling. DSS modulated ER-associated signaling in vivo and in vitro, accompanied by attenuation of pro-inflammatory transcriptional programs and enhancement of restoration-associated gene expression. Notably, ER antagonism markedly reversed the effect of DSS on microglial polarization, indicating that ER signaling is not merely an ancillary pathway but rather a critical upstream node required for DSS-driven microglial reprogramming. Together with prior evidence that ER signaling suppresses pro-inflammatory transcription and supports resolution and repair, our findings support a model in which DSS activates and/or depends on ER-linked transcriptional control to curb persistent inflammatory gene expression while promoting reparative programs, thereby establishing a microenvironment more permissive for white matter remodeling and remyelination and ultimately improving long-term neurological recovery during the post-stroke period.

A few considerations are important when interpreting these findings. (1) Microglial phenotypes were evaluated using established marker-based readouts, which may not fully capture the spectrum of microglial states in vivo. (2) DSS is a multi-component formulation; identifying key active constituents and confirming in vivo target engagement will further refine the mechanistic interpretation. (3) Microglia-specific ERα/ERβ loss-of-function and/or microglia depletion approaches will be pursued in follow-up studies to definitively establish cell-

type‐specific necessity and causality. (4) While our data support a microglia-centered mechanism, contributions from other cell types involved in white matter repair cannot be excluded. (5) Sex as a biological variable: Although estrogen receptor signaling was a mechanistic focus, the mechanistic experiments were performed in male mice. We initially conducted behavioral assessments in both male and female mice and observed no significant sex differences in baseline performance or in the behavioral response to DSS in our model (data not shown). Based on these results, and to reduce animal use and experimental complexity, we proceeded with male mice for subsequent mechanistic analyses. Nevertheless, we cannot exclude sex-specific effects at the cellular or molecular levels, and future studies will be needed to rigorously evaluate DSS efficacy and microglial ER signaling across sexes and hormonal states.

In summary, our study identifies DSS as a delayed, recovery-phase intervention that improves long-term outcome after transient focal cerebral ischemia. We propose that DSS promotes white matter repair by reprogramming microglia toward a reparative, pro-resolving state and by enhancing oligodendroglial differentiation through microglia-derived paracrine cues, with neurosteroid receptor signaling as a potential upstream regulatory axis. Overall, our results highlight microglia-directed modulation in the recovery phase as a tractable approach to promote white matter restoration and long-term functional improvement after stroke.

Acknowledgements

This work was supported by a by the National Natural Science Foundation of China (Grant No. 82274401, 82574915, 82371305).

Author contributions

C.R. and Y.Y. conceived and designed the study. C.R. and X.J. secured funding support. F.T. performed the majority of the experiments and analyzed the data. Y.L. and N.D. conducted part of the animal experiments. F.T. and C.R. drafted the manuscript. S.L., Z.H., and J.S. critically revised the manuscript. All authors reviewed and approved the final version of the manuscript.

Conflicts of interest

The authors have declared that no conflict of interest exists.

Supplementary Materials

The Supplementary data are available online at: www.aginganddisease.org/EN/10.14336/AD.2026.10202.

References

[1] Collaborators GBoCDaR (2025). Global, Regional, and National Burden of Cardiovascular Diseases and Risk Factors in 204 Countries and Territories, 1990-2023. J Am Coll Cardiol, 86:2167-2243.

[2] Wang Q, Liu N, Simo L, Ma Q, Li C (2025). A narrative review of reperfusion therapy in acute ischemic stroke: Emerging advances, current challenges, and future directions. Brain Circ, 11:187-199.

[3] Huuskonen MT, Wang Y, Nikolakopoulou AM, Montagne A, Dai Z, Lazic D, et al. (2022). Protection of ischemic white matter and oligodendrocytes in mice by 3K3A-activated protein C. J Exp Med, 219.

[4] Heo D, Kim AA, Neumann B, Doze VN, Xu YKT, Mironova YA, et al. (2025). Transcriptional profiles of mouse oligodendrocyte precursor cells across the lifespan. Nat Aging, 5:675-690.

[5] Tiwari V, Prajapati B, Asare Y, Damkou A, Ji H, Liu L, et al. (2024). Innate immune training restores pro-reparative myeloid functions to promote remyelination in the aged central nervous system. Immunity, 57:2173-2190.e2178.

[6] Shi L, Sun Z, Su W, Xu F, Xie D, Zhang Q, et al. (2021). Treg cell-derived osteopontin promotes microglia-mediated white matter repair after ischemic stroke. Immunity, 54:1527-1542.e1528.

[7] Deng Q, Wu C, Parker E, Liu TC, Duan R, Yang L (2024). Microglia and Astrocytes in Alzheimer's Disease: Significance and Summary of Recent Advances. Aging Dis, 15:1537-1564.

[8] Shi X, Zhang L, Wu S, Zhang C, Mamtilahun M, Li Y, et al. (2025). A simple polydopamine-based platform for engineering extracellular vesicles with brain-targeting peptide and imaging probes to improve stroke outcome. J Extracell Vesicles, 14:e70031.

[9] Zhao Q, Li J, Feng J, Wang X, Liu Y, Wang F, et al. (2025). Cholesterol metabolic reprogramming mediates microglia-induced chronic neuroinflammation and hinders neurorestoration following stroke. Nat Metab, 7:2099-2116.

[10] Yilmaz C, Karali K, Fodelianaki G, Gravanis A, Chavakis T, Charalampopoulos I, et al. (2019). Neurosteroids as regulators of neuroinflammation. Front Neuroendocrinol, 55:100788.

[11] Kalakh S, Mouihate A (2024). The Effects of Neuroactive Steroids on Myelin in Health and Disease. Med Princ Pract, 33:198-214.

[12] Wu SY, Chen YW, Tsai SF, Wu SN, Shih YH, Jiang-Shieh YF, et al. (2016). Estrogen ameliorates microglial activation by inhibiting the Kir2.1 inward-rectifier K(+) channel. Sci Rep, 6:22864.

[13] Saijo K, Collier JG, Li AC, Katzenellenbogen JA, Glass CK (2011). An ADIOL-ERβ-CtBP transrepression pathway negatively regulates microglia-mediated inflammation. Cell, 145:584-595.

[14] Lucchi C, Codeluppi A, Filaferro M, Vitale G, Rustichelli C, Avallone R, et al. (2023). Human Microglia Synthesize Neurosteroids to Cope with Rotenone-Induced Oxidative Stress. Antioxidants (Basel), 12.

[15] Yang Y, Li X, Chen G, Xian Y, Zhang H, Wu Y, et al. (2023). Traditional Chinese Medicine Compound (Tongxinluo) and Clinical Outcomes of Patients With Acute Myocardial Infarction: The CTS-AMI Randomized Clinical Trial. Jama, 330:1534-1545.

[16] Zhong LL, Zheng Y, Lau AY, Wong N, Yao L, Wu X, et al. (2022). Would integrated Western and traditional Chinese medicine have more benefits for stroke rehabilitation? A systematic review and meta-analysis. Stroke Vasc Neurol, 7:77-85.

[17] Itoh T, Michijiri S, Murai S, Saito H, Nakamura K, Itsukaichi O, et al. (1996). Regulatory effect of danggui-shaoyao-san on central cholinergic nervous system dysfunction in mice. Am J Chin Med, 24:205-217.

[18] Higaki S, Toyomoto T, Morohashi M (2002). Seijo-bofu-to, Jumi-haidoku-to and Toki-shakuyaku-san suppress rashes and incidental symptoms in acne patients. Drugs Exp Clin Res, 28:193-196.

[19] Qin L, Kamash P, Yang Y, Ding Y, Ren C (2024). A narrative review of potential neural repair poststroke: Decoction of Chinese angelica and peony in regulating microglia polarization through the neurosteroid pathway. Brain Circ, 10:5-10.

[20] Pu F, Mishima K, Egashira N, Akiyoshi Y, Liu AX, Sano K, et al. (2005). Post-ischemic treatment with toki-shakuyaku-san (tang-gui-shao-yao-san) prevents the impairment of spatial memory induced by repeated cerebral ischemia in rats. Am J Chin Med, 33:475-489.

[21] Chen G, Han M, Chen Y, Lei Y, Li M, Wang L, et al. (2023). Danggui-Shaoyao-San Promotes Amyloid-β Clearance through Regulating Microglia Polarization via Trem2 in BV2 Cells. J Integr Neurosci, 22:72.

[22] Ren C, Wang B, Li N, Jin K, Ji X (2015). Herbal Formula Danggui-Shaoyao-San Promotes Neurogenesis and Angiogenesis in Rat Following Middle Cerebral Artery Occlusion. Aging Dis, 6:245-253.

[23] Li S, Yang Y, Zhang W, Li H, Yu W, Gao C, et al. (2022). Systematic Understanding of Mechanism of Danggui Shaoyao San against Ischemic Stroke Using a Network Pharmacology Approach. Evid Based Complement Alternat Med, 2022:3747285.

[24] Li H, Yu W, Yang Y, Li S, Xu J, Gao C, et al. (2024). Combination of Atractylenolide I, Atractylenolide III, and Paeoniflorin promotes angiogenesis and improves neurological recovery in a mouse model of ischemic Stroke. Chin Med, 19:3.

[25] Qin L, Yang Y, Zhang H, Li S, Wu X, Wang M, et al. (2025). Hypoxic Preconditioning Mitigates Acute Hypoxia Induced MS/VDB Cholinergic Cell Loss and Memory Impairments. Aging Dis.

[26] Li N, Ren C, Li S, Yu W, Jin K, Ji X (2023). Remote ischemic conditioning alleviates chronic cerebral hypoperfusion-induced cognitive decline and synaptic dysfunction via the miR-218a-5p/SHANK2 pathway. Prog Neurobiol, 230:102514.

[27] Zhang W, Ren C, Yang Y, Xu J, Tong F, Wu X, et al. (2024). Ginseng aconitum decoction (Shenfu Tang) provides neuroprotection by ameliorating impairment of blood-brain barrier in cerebral ischemia-reperfusion injury. Brain Res, 1842:149098.

[28] Olszówka SC, Frey BM, Feldheim JF, Frontzkowski L, Wróbel PP, Backhaus W, et al. (2025). Localized network damage related to white matter hyperintensities is linked to worse outcome after severe stroke. Neurol Res Pract, 7:57.

[29] Taylor KR, Monje M (2023). Neuron-oligodendroglial interactions in health and malignant disease. Nat Rev Neurosci, 24:733-746.

[30] Guan J, Zhou W, Hafner M, Blake RA, Chalouni C, Chen IP, et al. (2019). Therapeutic Ligands Antagonize Estrogen Receptor Function by Impairing Its Mobility. Cell, 178:949-963.e918.

[31] Della-Flora Nunes G, Osso LA, Haynes JA, Conant L, Thornton MA, Stockton ME, et al. (2025). Incomplete remyelination via therapeutically enhanced oligodendrogenesis is sufficient to recover visual cortical function. Nat Commun, 16:732.

[32] Mollon JD, Takahashi C, Danilova MV (2022). What kind of network is the brain? Trends Cogn Sci, 26:312-324.

[33] Sagnier S, Catheline G, Dilharreguy B, Linck PA, Coupé P, Munsch F, et al. (2020). Normal-Appearing White Matter Integrity Is a Predictor of Outcome After Ischemic Stroke. Stroke, 51:449-456.

[34] Li W, He T, Shi R, Song Y, Wang L, Zhang Z, et al. (2021). Oligodendrocyte Precursor Cells Transplantation Improves Stroke Recovery via Oligodendrogenesis, Neurite Growth and Synaptogenesis. Aging Dis, 12:2096-2112.

[35] Yu X, Wu H, Zhao Y, Guo Y, Chen Y, Dong P, et al. (2018). Bone marrow mesenchymal stromal cells alleviate brain white matter injury via the enhanced proliferation of oligodendrocyte progenitor cells in focal cerebral ischemic rats. Brain Res, 1680:127-136.

[36] Li Y, Liu Z, Song Y, Pan JJ, Jiang Y, Shi X, et al. (2022). M2 microglia-derived extracellular vesicles promote white matter repair and functional recovery via miR-23a-5p after cerebral ischemia in mice. Theranostics, 12:3553-3573.

[37] Du W, Geng P, Lian Z, Sun Y, Zhou Y, Guo C, et al. (2025). DPSCs-Exos promote OPCs differentiation and white matter repair via Myl9-mediated PRMT5 nucleation after ischemic stroke. J Cereb Blood Flow Metab:271678x251399014.

[38] Ren Y, Zhao Y, Lu S (2013). Clinical Observation on Effect of Danggui Shaoyao Powder Combined with Rehabilitation Technique in Treatment of 60 Cases Cerebral infarction. JOURNAL OF LIAONING UNIVERSITY OF TCM, 15:210-211.

[39] Matsuoka T, Narumoto J, Shibata K, Okamura A, Taniguchi S, Kitabayashi Y, et al. (2012). Effect of toki-shakuyaku-san on regional cerebral blood flow in patients with mild cognitive impairment and Alzheimer's disease. Evid Based Complement Alternat Med, 2012:245091.

[40] Zhu Y, Wu Y (2021). Effect of Argatroban Combined with Danggui Shaoyao Powder on Acute Cerebral Infarction and Hemorheology. World Latest Medicine Information (Electronic Version), 21:261-263.

[41] Zhang H, Zhou LQ, Yang S, Dong MH, Chen L, Lu YL, et al. (2025). The foam cell-derived exosomes exacerbate ischemic white matter injury via transmitting metabolic defects to microglia. Cell Metab, 37:1636-1654.e1610.

[42] Hou X, Qu X, Chen W, Sang X, Ye Y, Wang C, et al. (2024). CD36 deletion prevents white matter injury by modulating microglia polarization through the Traf5-MAPK signal pathway. J Neuroinflammation, 21:148.

[43] Ma Y, Wang J, Wang Y, Yang GY (2017). The biphasic function of microglia in ischemic stroke. Prog Neurobiol, 157:247-272.

[44] Ji XY, Guo YX, Wang LB, Wu WC, Wang JQ, He J, et al. (2024). Microglia-derived exosomes modulate myelin regeneration via miR-615-5p/MYRF axis. J Neuroinflammation, 21:29.

[45] Raffaele S, Lombardi M, Marangon D, Abbracchio MP, Lecca D, Verderio C, et al. (2025). Microglia-Derived Extracellular Vesicles Enhance Oligodendrocyte Maturation by Transcriptionally Regulating Mitochondrial Molecular Pathways. Cell Mol Neurobiol, 45:89.

[46] Ghoumari AM, Abi Ghanem C, Asbelaoui N, Schumacher M, Hussain R (2020). Roles of Progesterone, Testosterone and Their Nuclear Receptors in Central Nervous System Myelination and Remyelination. Int J Mol Sci, 21.

[47] Qu Y, Li N, Xu M, Zhang D, Xie J, Wang J (2022). Estrogen Up-Regulates Iron Transporters and Iron Storage Protein Through Hypoxia Inducible Factor 1 Alpha Activation Mediated by Estrogen Receptor β and G Protein Estrogen Receptor in BV2 Microglia Cells. Neurochem Res, 47:3659-3669.

[48] Cordeau P, Jr., Lalancette-Hébert M, Weng YC, Kriz J (2016). Estrogen receptors alpha mediates postischemic inflammation in chronically estrogen-deprived mice. Neurobiol Aging, 40:50-60.

[49] Acosta-Martínez M (2020). Shaping Microglial Phenotypes Through Estrogen Receptors: Relevance to Sex-Specific Neuroinflammatory Responses to Brain Injury and Disease. J Pharmacol Exp Ther, 375:223-236.